IEEE Sensors Letters Volume 2(3) (2017)
Sensor phenomena

Screen-printed resistivity sensor for in-situ and real-time monitoring of concrete moisture content suitable for smart buildings/cities and IoT

Marios Sophocleous[1], Pericles Savva[2], Michael F. Petrou[2], John K. Atkinson[3] and Julius Georgiou[1]*

[1] *Holistic Electronics Research Laboratory, Department of Electrical and Computer Engineering, University of Cyprus, Nicosia, Cyprus*
[2] *Department of Civil and Environmental Engineering, University of Cyprus, Nicosia, Cyprus*
[3] *Faculty of Engineering and the Environment, University of Southampton, Southampton, UK*
** Senior Member, IEEE*

Received 1 Nov 2016, revised 25 Nov 2016, accepted 30 Nov 2016, published 5 Dec 2016, current version 15 Dec 2016. (Dates will be inserted by IEEE; "published" is the date the accepted preprint is posted on IEEE Xplore®; "current version" is the date the typeset version is posted on Xplore®).

Abstract—This paper shows initial experimental results on the utilization of a low-cost, screen-printed resistivity sensor in concrete, with the aim of monitoring concrete moisture content in real-time. The sensor was tested in two different concrete types, one with high-absorptive aggregates (5.1%) and one with low-absorptive aggregates (1.0%). Initial experimental results show a significant correlation of the sensor's response and the moisture content of concrete, with the sensor being capable of distinguishing between different concrete types by their different drying rates. The sensor recorded very similar resistivity rates as those found in the literature with modelled sensor outputs of ρ=45.86+109.7+ln (t) and ρ=0.691+8.11*ln (t) for low-absorptive and high-absorptive mixtures, respectively. This sensor features the ability to be easily integrated in a structure management system employed within smart buildings and smart cities. These correlations of concrete resistivity with water content can provide vital information regarding key properties of concrete whose monitoring may contribute to more durable structures by the implementation of preventative maintenance rather than reactive maintenance.

Index Terms—Concrete resistivity, concrete moisture content, resistivity sensor, screen-printing, sensor phenomena.

I. INTRODUCTION

Routine monitoring and health inspection of civil infrastructures such as bridges, overpasses, and buildings are vital in order to ensure public safety. In 2005, according to the Bureau of Transportation Statistics (BTS), approximately 26.2% of the bridges in the USA were designated as structurally deficient/obsolete [1]. Most common causes of bridge failure/deterioration are floods and collisions [2] therefore, the National Bridge Inspection Program has requested the collection of field data for proper rehabilitation and maintenance [3].

Strength and durability of concrete depend on temperature, ion concentrations and the dynamics of ion and moisture transport [4], [5]. The material properties of concrete and steel rebars change with time and these properties are significantly influenced by the heat of hydration, temperature, ion transport and moisture content of concrete at early ages [6]. Moisture diffusion during curing may prevent concrete from developing its full strength and it might also lead to high shrinkage stresses [7]. Deterioration mechanisms of structures such as bridges and buildings are very closely related to their moisture and temperature characteristics but also depend on environmental conditions [8].

Deterioration mechanisms of concrete are well known and the most important are chloride penetration and carbonation. Several sensors have been reported for monitoring the concentration of chloride and carbon dioxide [9], [10]. These two deterioration mechanisms induce steel oxidation, which decreases the strength and durability of the structure [11], [12]. A key parameter that plays a very important role in concrete deterioration is the moisture content. Increased levels of moisture content can accelerate both of the above-mentioned mechanisms. In addition, concrete features its best performance at certain moisture content levels.

Currently, in most cases, structural health monitoring is done by using Ground Penetrating Radars (GPR), a technique that is time consuming, labor intensive and costly, eliminating its suitability in real-time systems [3], [13]. The recent concept of implementing the Internet of Things (IoT) within smart cities and buildings has created the need for real-time sensors to monitor the condition of important structures such as bridges and skyscrapers [5]. Real-time condition monitoring of concrete has been under extensive investigation during the last decade [14].

Several moisture content sensors including fibre optic and fibre grating [15]–[18], redox potential [19], hand-held NMR [20], interdigitated near-field [3], MEMS and NEMS [5] and passive RFID sensors [14] have been reported within the last decade but their manufacturing and instrumentation costs are rather high (>€150), which does not allow their implementation in everyday structures [21], [22].

In this paper, a low-cost, screen-printed sensor is described that is

Corresponding author: M. Sophocleous (sophocleous.marios@ucy.ac.cy).
Digital Object Identifier: 10.1109/LSEN.XXXX.XXXXXXX (inserted by IEEE).

cheap enough to allow its implementation even in residential buildings with the ability to be implanted in concrete during construction and provide real-time readings for an extended period of time. The sensor itself can cost less than €10 whilst its instrumentation can cost less than €15, when mass-produced. This price range allows the immersion of the sensor in concrete during construction and it has the unique ability to include sensors for other parameters on the same substrate in the future.

II. SENSOR FABRICATION

The sensor's operating principle is based on the classical four electrodes method of resistivity measurement. The conventional four electrodes method is very simple and well known and more details can be found elsewhere [23].

The sensor was fabricated using Thick-Film Technology and the electrode layers were printed on two 50 mm × 25 mm, 0.625 mm thick, 96% alumina substrates (Coorstech). The inks were printed using stainless steel screens with a mesh count of 250 lines per inch, 15 µm emulsion thickness and a 45º mesh. The screen designs for each layer were created on AUTOCAD and were manufactured by MCI Cambridge for the Aurel C880 Printer.

The first layer printed on the alumina substrate was the gold conductor with three rectangular screen mesh openings and dimensions of 4.5 mm × 45 mm. A waterproofing layer was printed on top of the gold electrodes, with a rectangular shape of 6.5 mm × 14 mm to leave an exposed electrode area of 26 mm × 4.5 mm. The distance between the electrodes of the same substrate was approximately 4.5 mm. Wires were soldered on one end of the gold electrodes, with the exposed solderable area being approximately 5 mm × 4.5 mm in dimension. The gold electrodes were printed using ESL 8844 ink (Electro Science) and the glass dielectric insulator was printed using ESL 4905-C (Electro Science) to expose a precise surface area of the electrodes. The individual sensor layers were printed and cured sequentially with the specific printing and curing procedure and temperatures as described previously [24]. A schematic of a single substrate with the printed layers is shown in Fig. 1 below.

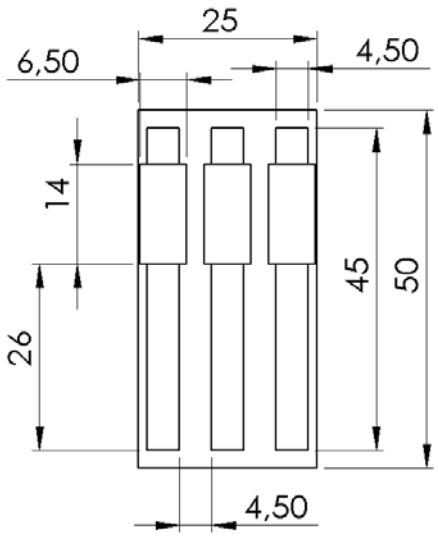

Fig. 1. Design of the electrodes on one substrate.

The sensor was constructed by placing two identical substrates, with three electrodes on each substrate, facing each other with a spacing distance between opposite electrodes of 10 mm. The sensor was designed such that the drive current is applied across the two outer sets of electrodes, while the resulting potential across the cell is measured by the inner electrode on each substrate [25]. The final construction of the sensor is shown in Fig. 2 below.

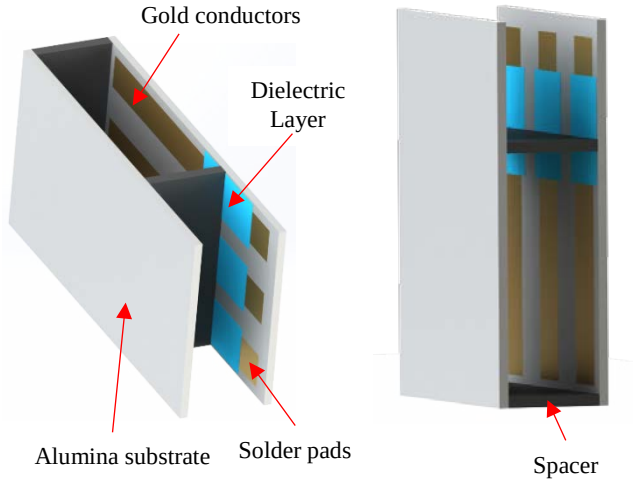

Fig. 2. Construction of the screen-printed resistivity sensor.

This electrode geometry was specifically used to minimize any field fringing effects and to eliminate the susceptibility of the sensor to rotational movements of each individual substrate. Based on the theory of the classical four-electrode method, the resistivity of the material between the two substrates will be proportional to the voltage measured across the inner voltage electrode pair.

Further information on the construction, operation and performance of the sensor can be found in an earlier publication [24].

III. EXPERIMENTAL SETUP

Two concrete mixtures (Type 1 (T1) and Type 2 (T2)) with low water/concrete ratio (0.25) were designed. The mixtures' constituents are shown in Table 1.

Table 1: Concrete mixtures constituents

	TYPE 1 (kg/m^3)	**TYPE 2** (kg/m^3)
CEMENT (CEM 52.5R)	864	864
Water	216	216
Coarse (Limestone- 4/10mm)	854	854
Sand (Limestone- 0/4mm)	499	383
Internal Curing Water	-	44

The aggregates utilized in both types of concrete were limestone from local quarries. The aggregates utilized were low-absorptive (1.0%) for the T1 mixture and high-absorptive (5.1%) for the T2 mixture. Mixture T2 was designed to be cured internally using the water carried in the aggregates' pores. Internal curing refers to a

technique used in concrete technology that reduces self-desiccation of concrete. Self-desiccation is an intrinsic characteristic of cement paste, which occurs during solidification when the quantity of water is not sufficient for full hydration. The relative humidity drop occurs due to the lack of water. The mechanism of internal curing provides water from the inner structure to replenish the consumed water and maintain relative humidity at high levels. More information about the internal curing mechanism and the aggregates' mechanical and mineralogical properties can be found elsewhere [26], [27].

The mixtures were prepared in a horizontal rotary mixing machine. The aggregates were utilized to evaluate their effectiveness as internal curing agents [27]. The concrete mixtures were cast in a plastic non-absorptive mold of dimensions 100 mm x 100 mm x 100 mm. The experiments on specimen T1 were performed in laboratory conditions without any insulation whilst specimen T2 was insulated with a plastic membrane to prevent moisture loss and with an extruded polystyrene (XPS) box with a lambda value in the range 0.029 to 0.039 ($Wm^{-1}K^{-1}$) to simulate adiabatic conditions (Fig. 3).

Fig. 3. Concrete cube in the polystyrene box.

The sensor employed an alternating square wave current source of 1 mA at a frequency of 1 kHz, which is low enough to measure resistivity independently of any electrode capacitance but high enough to prevent any polarization effects on the electrodes. The voltage was logged using a commercial data logger (Campbell Scientific CR1000) with a sampling rate of 0.1 s^{-1}.

The two concrete blocks were developed at different times and dates and left to dry over a period of 9 days.

IV. RESULTS & DISCUSSION

The data logger recorded voltage with respect to time, for a given drive current (A), hence the measured resistance R (Ω) is obtained by applying Ohm's Law.

Hence, the resistivity ρ (Ω m) of the sample is calculated as:

$$\rho = R\left(\frac{A}{L}\right) \quad (1)$$

where A/L is the cell constant of the sensor (m), with A being the cross sectional area of the cell (m^2) and L the distance between opposite facing electrodes (m).

The measured voltages have been translated to resistivity values based on the assumption that the cell constant of the sensor does not change significantly within the measured resistivity range. Based on the sensor's performance in previous experiments [24], the cell constant was assumed equal to the calculated geometrical value of 0.0611 meters within the range of resistivity values obtained here.

Fig. 4 below shows the resistivity data obtained from the sensor for both concrete types, during a 9-day period. The graphs were plotted using Matlab® software.

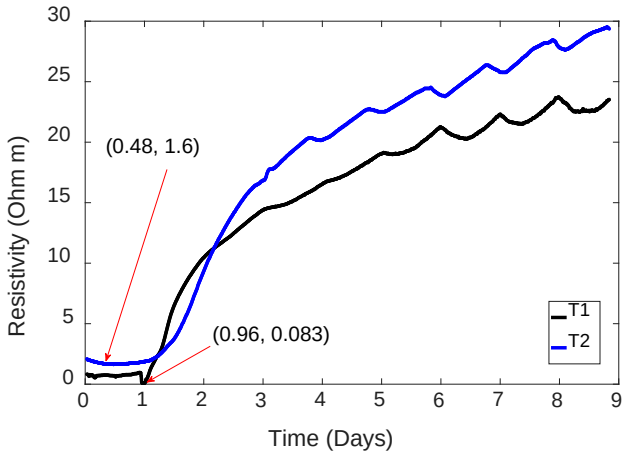

Fig. 4. Sensor output for the two concrete types showing the minimum resistivity points.

Initially, during the concrete's liquid form, the moisture-content of the mixture is at its highest; as the water-molecules are consumed in hydration products, the resistivity of the mixture increases. Moisture content reaches an equilibrium point that depends on the relative humidity of the environment. The obtained resistivity change profile is consistent with the trend identified in [28], which was obtained by taking resistivity measurements with commercial sensors and very similar methods.

Resistivity measurements are significantly dependant on temperature even if concrete water content is the same. Thus, existing commercially available resistivity probes incorporate linear and non-linear temperature compensation algorithms. This effect can be clearly observed in Fig. 4, where periodic resistivity fluctuations with a period of 24 hours due to environmental temperature fluctuations between day and night can be observed. The fluctuations are more evident for T1 sample because the polystyrene box was only used for the T2 sample and the sensor was more exposed to temperature changes. Although temperature can affect the sensor's readings, the recorded resistivity changes are an order of magnitude higher than those observed from temperature changes, which suggests that the resistivity changes are mostly due to changes in water content.

It was initially expected that the resistivity of T1 would be much higher than T2 due to internal curing of T2, retaining higher amounts of water. However, from Fig. 4 the resistivity of T1 is actually lower after the 9-day period. Resistivity of concrete can be affected not only by the water content but also by the concentration and mass transport dynamics of charge carriers/ions within the mixture. Therefore, in order to eliminate the difference between charge carrier concentrations in the two concrete types, their resistivity was normalised using the lowest resistivity point of each concrete type.

The obtained normalised resistivity results are plotted in Fig. 5 and fitted curves were obtained using Matlab® software. The initial resistivity readings of both types are omitted from Fig. 5 to allow better curve fitting and hence modelling of the drying rates.

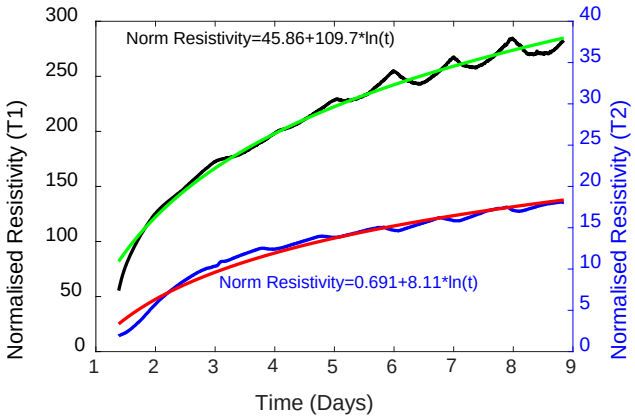

Fig. 5. Normalised resistivity values of the two concrete types.

Fig. 5 shows that T1 changes its resistivity value by almost 300 times while T2 changes its resistivity value by almost 20 times in the same time period suggesting that although the absolute resistivity values of the two concrete types are similar, there is a major difference in their resistivity changes during the tested period.

These results suggest that each concrete type could possibly have its own unique curve equation. In addition, the rate and the extent of hydration, are expected to be different due to internal curing, which will most probably have an effect on the obtained drying rate models.

V. CONCLUSIONS

This paper demonstrates a low-cost, screen-printed resistivity sensor capable of monitoring the moisture content of concrete in real-time. The sensor is suitable for application to smart structures and can be integrated in multiple IoT applications. Obtained results are in-line with data from the literature and they further suggest that monitoring the resistivity of the concrete in its initial and later stages, can distinguish between different concrete types, whilst allowing for predictive maintenance instead of reactive.

Further work is in progress to compare the sensor's output with resistivity and moisture content as measured with other techniques and/or commercially available equipment in parallel. In addition, more concrete types are in line to be tested to compare the sensor's performance in order to fully calibrate and characterise the sensor. Future experiments will be performed in controlled environmental chambers to control both air humidity and temperature. Furthermore, temperature compensation algorithms are in process to be implemented in order to eliminate any errors arising from temperature fluctuations.

REFERENCES

[1] D. of T. U. S. Bureau of Transportation Statistics, "Road Bridge Condition: 2005," 2005. [Online]. Available: https://www.bts.gov/archive/publications/state_transportation_statistics/state_transportation_statistics_2006/table_01_07.

[2] K. Wardhana and F. C. Hadipriono, "Analysis of Recent Bridge Failures in the United States," *J. Perform. Constr. Facil.*, vol. 17, no. 3, pp. 144–150, 2003.

[3] M. N. Alam, R. H. Bhuiyan, R. A. Dougal, and M. Ali, "Concrete moisture content measurement using interdigitated near-field sensors," *IEEE Sens. J.*, vol. 10, no. 7, pp. 1243–1248, 2010.

[4] J. N. Eiras, T. Kundu, J. S. Popovics, J. Monzo, M. V. Borrachero, and J. Paya, "Effect of carbonation on the microstructure and the moisture properties of cement-based materials," in *Optique Engineering*, 2016, vol. 55, no. 1, pp. 1–8.

[5] A. Norris, M. Saafi, and P. Romine, "Temperature and moisture monitoring in concrete structures using embedded nanotechnology/microelectromechanical systems (MEMS) sensors," *Constr. Build. Mater.*, vol. 22, no. 2, pp. 111–120, 2008.

[6] J. K. Kim and C. S. Lee, "Moisture diffusion of concrete considering self-desiccation at early ages," *Cem. Concr. Res.*, vol. 29, no. 12, pp. 1921–1927, 1999.

[7] B. person and G. Fagerlund, "Self-Desiccation and Its Importance in Concrete Technologu," *Rep. TVBM-3075*, vol. 30, no. 1, pp. 1–261, 1997.

[8] A. M. Neville, *Properties of Concrete*, vol. Fourth. 2011.

[9] J. M. Gandia-Romero *et al.*, "Characterization of embeddable potentiometric thick-film sensors for monitoring chloride penetration in concrete," *Sensors Actuators, B Chem.*, vol. 222, pp. 407–418, 2016.

[10] W. J. McCarter and Ø. Vennesland, "Sensor systems for use in reinforced concrete structures," *Constr. Build. Mater.*, vol. 18, no. 6, pp. 351–358, 2004.

[11] H. M.A.AL-Mattarneh, "Microwave Sensing of Moisture Content in Concrete Using Open-ended Rectangular Waveguide," *Subserface Sens. Technol. Appl.*, vol. 2, no. 4, 2001.

[12] I. Martínez and C. Andrade, "Examples of reinforcement corrosion monitoring by embedded sensors in concrete structures," *Cem. Concr. Compos.*, vol. 31, no. 8, pp. 545–554, 2009.

[13] C. Maierhofer, "Nondestructive Evaluation of Concrete Infrastructure with Ground Penetrating Radar," vol. 15, no. June, pp. 287–297, 2003.

[14] J. B. Ong, Z. Y. Z. You, J. Mills-Beale, E. L. T. E. L. Tan, B. D. Pereles, and K. G. O. K. G. Ong, "A Wireless, Passive Embedded Sensor for Real-Time Monitoring of Water Content in Civil Engineering Materials," *IEEE Sens. J.*, vol. 8, no. 12, pp. 2053–2058, 2008.

[15] T. L. Yeo, D. Eckstein, B. McKinley, L. F. Boswell, T. Sun, and K. T. V Grattan, "Demonstration of a fibre-optic sensing technique for the measurement of moisture absorption in concrete," *Smart Mater. Struct.*, vol. 15, no. 2, pp. 39–45, 2006.

[16] K. Bremer *et al.*, "Fibre Optic Sensors for the Structural Health Monitoring of Building Structures," *Procedia Technol.*, vol. 26, pp. 524–529, 2016.

[17] T. L. Yeo, M. A. C. Cox, L. F. Boswell, T. Sun, and K. T. V Grattan, "Optical fiber sensors for monitoring ingress of moisture in structural concrete," *Rev. Sci. Instrum.*, vol. 77, no. 5, 2006.

[18] S. Zheng, "Long-period fiber grating moisture sensor with nano-structured coatings for structural health monitoring," *Struct. Heal. Monit. An Int. J.*, vol. 14, no. 2, pp. 148–157, 2015.

[19] S. Muralidharan, T. H. Ha, J. H. Bae, Y. C. Ha, H. G. Lee, and D. K. Kim, "A promising potential embeddable sensor for corrosion monitoring application in concrete structures," *Meas. J. Int. Meas. Confed.*, vol. 40, no. 6, pp. 600–606, 2007.

[20] P. J. Prado, "NMR hand-held moisture sensor," *Magn. Reson. Imaging*, vol. 19, no. 3–4, pp. 505–508, 2001.

[21] B. Han, X. Yu, and E. Kwon, "A self-sensing carbon nanotube/cement composite for traffic monitoring," *Nanotechnology*, vol. 20, no. 44, p. 445501, 2009.

[22] M. Chiarello and R. Zinno, "Electrical conductivity of self-monitoring CFRC," *Cem. Concr. Compos.*, vol. 27, no. 4, pp. 463–469, 2005.

[23] M. N. Nabighian, *Electromagnetic Methods in Applied Geophysics, Theory, vol.1*. 2006.

[24] M. Sophocleous and J. K. Atkinson, "A novel thick-film electrical conductivity sensor suitable for liquid and soil conductivity measurements," *Sensors Actuators, B Chem.*, vol. 213, pp. 417–422, 2015.

[25] J. K. Atkinson and M. Sophocleous, "A novel thick-film screen printed electrical conductivity sensor for measurement of liquid and soil conductivity," *IEEE SENSORS 2014 Proc.*, pp. 86–89, 2014.

[26] A. P. Savva, G. D. Nicolaides, and F. M. Petrou, "High Absorptive Normal Weight Aggregates Used as Internal Curing Agents to Reduce Hot Weather Concreting and Curing Detrimental Effects," *Key Eng. Mater.*, vol. 711, no. September, pp. 420–427, 2016.

[27] P. Savva and M. Petrou, "High-Absorptive Normal-Weight Aggregates used as Internal Curing Agent," in *27th Bienn. Natl. Conf. Concr. Inst. Aust. Conjuction with 69th RILEM Week*, 2015, pp. 1305–1313.

[28] D. Bjegović *et al.*, "Test Methods for Concrete Durability Indicators," in *Performance-Based Specifications and Control of Concrete Durability*, 2016, pp. 51–105.